Science of the Total Environment 966 (2025) 178725

Contents lists available at ScienceDirect

Science of the Total Environment

journal homepage: www.elsevier.com/locate/scitotenv

Validation of the spray drift modeling software AGDISPpro applied to remotely piloted aerial application systems

Sebastian Castro-Tanzi [a,*], Michael Winchell [a], Zhenxu Tang [b], Milton E. Teske [c], Glen R. Whitehouse [c], Brad Fritz [d], Dan Martin [d]

[a] Stone Environmental Inc., USA
[b] Environmental Exposure Modeling, Regulatory Science North America, Bayer US Crop Science Division, Chesterfield 63017, USA
[c] Continuum Dynamics, Inc.
[d] USDA Agricultural Research Service, Aerial Application Technology Research, College Station, TX, USA

HIGHLIGHTS

- AGDISPpro combines atmospheric transport and multi-rotor aerodynamic models
- AGDISPpro predicts off-target spray drift from drones (RPAAS)
- Eighteen drone applications with varying spray quality were simulated in AGDISPpro
- Predicted in-field and off-target depositions matched well with field observations
- Swath width and displacement inputs led to discrepancies in deposition predictions

GRAPHICAL ABSTRACT

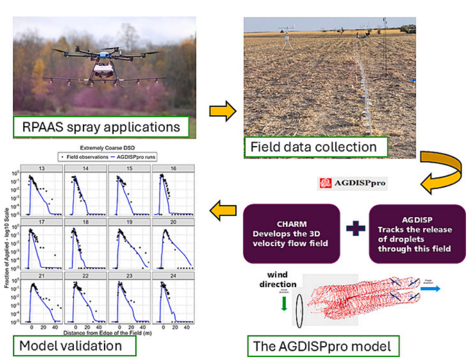

ARTICLE INFO

Editor: Jay Gan

Keywords:
Spray drift deposition
Spray drift modeling
Drone
Pesticide applications
Agriculture

ABSTRACT

Regulatory bodies worldwide are currently developing modeling frameworks to simulate pesticide drift following applications from remotely piloted aerial application systems (RPAAS). Unfortunately, there are no currently validated mechanistic models that simulate off-target droplet movement from these systems. To respond to this modeling gap, we evaluated AGDISPpro, an established Lagrangian-based drift and deposition model following applications by fixed and rotary wing aircraft. Specifically, we evaluated two of the nine RPAAS models available in AGDISPpro, i.e., PV22 quadcopter and PV35X hexacopter models. Our detailed evaluation relied on two sets of field studies: a series of single-swath applications using medium and extremely coarse spray nozzles, and a series of four-swath applications using fine and ultra coarse spray nozzles. AGDISPpro model predictions were compared to in-swath and downwind deposition measurements. The r index of agreement ranged from 0.47 to 0.92 for medium nozzles, 0.61–0.94 for extremely coarse nozzles, and from 0.86 to 0.93 to 0.48–0.55 for fine and ultra-coarse nozzles respectively. There is uncertainty regarding how swath width and swath displacement behavior from the RPAAS affect the location, width, and magnitude of the peak deposition and deposition plume.

* Corresponding author.
E-mail address: scastro@stone-env.com (S. Castro-Tanzi).

https://doi.org/10.1016/j.scitotenv.2025.178725
Received 18 November 2024; Received in revised form 31 January 2025; Accepted 2 February 2025
Available online 8 February 2025

Thus, further research is required to reduce this uncertainty. Overall, this study demonstrates that AGDISPpro is a promising tool for modeling off-target spray deposition effects from RPAAS.

1. Introduction

1.1. RPAAS applications of pesticides

The integration of Remotely Piloted Aerial Application Systems (RPAAS) into agricultural practices marks a significant technological advance in crop management and protection strategies. Originally developed for military applications (Sharkey, 2011; Konert and Balcerzak, 2021), RPAASs have found a new and rapidly growing place in agriculture, driven by the need for more efficient and precision farming practices (Kaivosoja, 2022; Radoglou-Grammatikis et al., 2020). Among the many benefits of RPAAS applications for agriculture, their flexibility, lower operational costs, reduced operator exposure, and the ability to access difficult terrains have made RPAAS particularly attractive for chemical spraying (Yan et al., 2021; Kuster et al., 2023; Felkers et al., 2024; Weicai and Panya, 2023; Zhang et al., 2023; Hassler and Baysal-Gurel, 2019). In the past decade, chemical application by the RPAAS spraying technologies have been widely adopted in East Asian regions with rapidly increasing worldwide adoption (Zhou, 2013; Zhang et al., 2023; Dubuis et al., 2023). By reducing the quantity of chemicals used and minimizing their impact on the environment, RPAAS contribute to lower economic and environmental costs, and help in the move towards sustainable agricultural practices (Martinez-Guanter et al., 2020; Sahni et al., 2024).

The phenomenal growth of RPAAS has raised environmental and regulatory questions on off-target pesticides loss through spray drift. Spray drift is the movement of pesticide droplets away from the target area to any off-target location during the spray operation or shortly thereafter (Nuyttens et al., 2007; Wang et al., 2020b). Wind speed and direction can significantly influence the trajectory of pesticide droplets. Temperature and humidity also affect droplet evaporation rates and, consequently, the likelihood of drift. In addition, vehicular speed, wake, droplet release height, spray volume, and nozzle orifice are critical factors influencing spray drift. The effects of these factors on spray drift from conventional aerial and ground applications are well understood due to wind tunnel studies, field trials, and physical-based spray drift models. Spray drift in the context of RPAAS is being actively studied by researchers through wind tunnel and field studies (Wang et al., 2020a; Wang et al., 2021; Zhang et al., 2023; Wongsuk et al., 2024; Bonds, 2022; Bonds et al., 2023; Glaser et al., 2020; Herbst et al., 2020; Martin et al., 2025). Advances in technologies have made it possible for RPAAS manufacturers to produce a wide range of models of different sizes, weights and shapes, and capable of carrying different sensor payloads (del Cerro et al., 2021, Guebsi et al., 2024). There is a need for mechanistic spray drift models for RPAAS due to the large number of different configurations and operating practices that make field studies and empirical models cost prohibitive (OECD, 2021). AGDISPpro is a mechanistic model used to predict spray drift deposition from aerial applications. The latest version currently integrates RPAAS aerodynamic flow-field models (Teske et al., 2018a, 2018b). However, AGDISPpro predictions of spray drift deposition from RPAAS have not been validated in the scientific literature (Teske and Whitehouse, 2024). Therefore, conducting such validation is key to determining if AGDISPpro can be used to accurately model spray drift from RPAAS.

1.2. Mechanistic spray drift modeling of pesticides

In the 1970s, a Gaussian plume dispersion modeling initiative, and a parallel characterization of the atmospheric boundary layer, were adopted by the US Environmental Protection Agency to calculate the concentrations of an airborne pollutant at specified distances from industrial sources (Teske et al., 2011b). Gaussian modeling tracks the dispersion of a cloud using a steady-state exponential formulation tying the strength of the cloud to the three directions of motion. For example, one of the simplest Gaussian formulations is that of the airborne concentration (χ, g m^{-3}) of a point release from an elevated source (Turner, 1994):

$$\chi = \frac{Q}{2\pi u \sigma_y \sigma_z} exp\left[-\frac{y^2}{2{\sigma_y}^2}\right]\left\{exp\left[-\frac{(H-z)^2}{2{\sigma_z}^2}\right] + exp\left[-\frac{(H+z)^2}{2{\sigma_z}^2}\right]\right\} \tag{1}$$

where Q is the emission rate (g s^{-1}), u is the wind speed at the point of release (m s^{-1}), σ_y is the lateral standard deviation of the cloud (m), σ_z is the vertical standard deviation of the cloud (m), y is the distance perpendicular to the along-wind distance (m), z is the height above the ground (m), and H is the release height (m). Although this equation is relatively simple, extending the Gaussian approach to more complicated problems rapidly introduces mathematical and numerical complexity.

Going forward, provision was made in the US Army's Gaussian modeling codes to account for the loss of material by gravitational settling of droplets from elevated spray clouds and to predict resulting surface deposition patterns using simplified line source models (Cramer et al., 1972). This early work demonstrated the feasibility of modeling as an operational tool and as a basis for research on pesticide application from aerial and ground platforms into plant and forest canopies. The model was eventually called FSCBG (Dumbauld et al., 1980) and was developed for the USDA Forest Service from models and work supported by the US Army at Dugway Proving Ground. FSCBG (for Forest Service Cramer Barry Grim, after its developers) included algorithms for considering the penetration of droplets into canopies and simple expressions for wake effects of spray aircraft, as well as an algorithm to consider evaporation of spray droplets (Teske et al., 1993b).

In 1979, the National Aeronautics and Space Administration (NASA) supported the initial development of a Lagrangian droplet trajectory model. The development of this technology was made technically feasible by previous research directed at understanding the physics of vortex wakes behind aircraft (i.e., Bilanin et al., 1977, 1978). A simple vortex wake model, patterned after an approach suggested by Reed (1953), and the subsequent development of a closure technique to recover the effect of atmospheric turbulence on the variance of the spray material about its mean trajectory (Houbolt et al., 1964; Teske et al., 2003), led to the development of the Lagrangian model AGDISP (AGricultural DISPersal) funded by the U. S. Department of Agriculture (USDA) Forest Service until September 2019. AGDISP is a widely used regulatory model in the US, specifically for the Environmental Protection Agency (USEPA), Canada (Pest Management Regulatory Agency), New Zealand, and Australia, among others (H.W. Thistle, 2024, personal communication). AGDISPpro is an enhancement of AGDISP, with additional modeling features implemented by Continuum Dynamics, Inc. (CDI). Licensing of the executable code is supported by Mount Rose Scientific, LLC (https://mount-rose.com). Over 40 technical and peer-reviewed publications detail the ongoing improvements to the model, as summarized in Teske and Whitehouse (2024) and documented in Bilanin et al. (1989) and Teske et al. (2003, 2011a, 2019). Modeling applications are discussed further in Thistle et al. (2020), Teske and Whitehouse (2022), and Teske et al. (2022).

1.3. Spray drift models for RPAAS applications

As RPAAS technology is being adopted at an accelerated pace globally, there is an urgent need from regulators to understand and quantitatively characterize spray drift from RPAAS applications. This information is necessary in risk assessments conducted for pesticide registration and to determine best spray practices (OECD, 2021).

AGDISPpro coupled with CHARM (Comprehensive Hierarchical Aeromechanics Rotorcraft Model) (Wachspress et al., 2003a) simulated wake flow fields to predict the deposition and drift released from RPAAS (Teske et al., 2018b). AGDISPpro tracks the motion of spray droplets released from nozzles using the Lagrangian approach for RPAAS wakes generated with CHARM. A detailed description of the model is provided in section 2.1. The CFD (Computational Fluid Dynamics) method, which solves complex airflow and turbulence patterns by resolving the Navier–Stokes equations, could also be used to model wakes from RPAAS (Miller and Hadfield, 1989; Yang et al., 2018). However, CFD simulation requires enormous computational resources and costs compared to other methods, such as CHARM. It also needs careful consideration of the trade-offs between the sizes of target areas, the desired accuracy of simulations, and the computational costs. Despite the complexity of the CFD approach, there have been interesting simulations, but the results indicated large errors between simulated and empirical values due to various factors (Weicai and Panya, 2023). To be useful, CFD simulations need to be more realistic and incorporate more aspects of the application process (OECD, 2021).

The primary objective of this research is to evaluate AGDISPpro's ability to simulate spray deposition from RPAAS through comparison to data from field studies. This objective was accomplished by: 1) Parameterization of the RPAAS component of AGDISPpro to represent specific RPAAS employed in two field studies; 2) Parametrization using meteorological, RPAAS operational conditions, and spray characteristics from each study; and 3) Comparison and statistical evaluation of AGDISPpro modeling results with field study results.

2. Materials and methods

2.1. AGDISPpro model development

2.1.1. Theory

AGDISPpro tracks the motion of spray droplets released from nozzles positioned on a spray boom, with one droplet released from each nozzle for each droplet size in the discretized drop size distribution. The Lagrangian approach partitions the variables into mean and fluctuating components [$X_i + x_i$ for droplet location (m), $V_i + v_i$ for droplet velocity (m s^{-1}), and $U_i + u_i$ for background velocity (m s^{-1}), where the indices are not summed] to give the equations:

$$\frac{d^2}{dt^2}(X_i + x_i) = [(U_i + u_i) - (V_i + v_i)]\left[\frac{1}{\tau_p}\right] + g_i \tag{2}$$

$$\frac{d}{dt}(X_i + x_i) = (V_i + v_i) \tag{3}$$

where t is time (s), X_i is the mean location of the droplet (m), x_i is the fluctuating location of the droplet (m), V_i is the mean velocity of the droplet (m s^{-1}), v_i is the fluctuating velocity of the droplet (m s^{-1}), U_i is the mean background velocity (m s^{-1}), u_i is the fluctuating background velocity (m s^{-1}), g_i is gravity (0, 0, $-g$) (m s^{-2}), and τ_p is the droplet relaxation time (s):

$$\tau_p = \frac{4}{3}\frac{\rho D}{C_D \rho_a |U_i - V_i|} \tag{4}$$

where ρ is the droplet density (kg m^{-3}), D is the droplet diameter (μm), C_D is the droplet drag coefficient (nondimensional), and ρ_a is the air density (kg m^{-3}). Equations governing the mean transport of a released droplet may then be written by ensemble averaging Eqs. 2 and 3:

$$\frac{d^2X_i}{dt^2} = [U_i - V_i]\left[\frac{1}{\tau_p}\right] + g_i \tag{5}$$

$$\frac{dX_i}{dt} = V_i \tag{6}$$

The drag coefficient C_D in Eq. 4 is evaluated empirically for spherical droplets (Langmuir and Blodgett, 1949) as:

$$C_D = \frac{24}{Re[1 + 0.197Re^{0.63} + 0.00026\,Re^{1.38}]} \tag{7}$$

where the Reynolds number is defined as:

$$Re = \frac{\rho_a D|U_i - V_i|}{\mu_a} \tag{8}$$

and μ_a is the viscosity of air (kg m^{-1} s^{-1}).

The fluctuation equations are obtained by subtracting Eqs. 5 and 6 from Eqs. 2 and 3, respectively, pre-multiplying appropriately by x_i and v_i, ensemble averaging, and manipulating, to yield equations involving position variance, droplet location and velocity correlation, and droplet velocity variance. The lengthy derivation of these correlations and the assumptions needed to resolve them may be found in Teske et al. (2003).

The droplet evaporation model is based on recent laboratory tests (Teske et al., 2018a):

$$1 - \frac{D^2}{D_O^2} = a\frac{t}{\tau_e}\left[1 + b\frac{t}{\tau_e}\right] \tag{9}$$

with the parameters $a = 0.2228$ and $b = 0.3136$ ($R^2 = 0.959$), where τ_e is the evaporation time scale (s).

2.1.2. Modeling RPAAS

In the present application, the AGDISPpro model follows the release of spray droplets into RPAAS wake flow fields generated with CHARM, a self-contained wing/rotor/wake/body computational analysis that models aircraft wing and rotor blade aerodynamics and dynamics in hover and forward flight. The model began with an initial description of the curved vortex element approach to the wake generated by a helicopter (Bliss et al., 1987a), extending to a large number of published and presented results, best represented by Quackenbush and Bliss (1988, 1990, 1991), Quackenbush et al. (1989, 1994, 1995, 1996, 2017), Wachspress et al. (2003a, 2003b, 2003c, 2009), Wachspress and Quackenbush (2006), and Whitehouse et al. (2007, 2018). These references include extensive model comparisons with laboratory, wind tunnel, and real-world field datasets.

A more complete description of the CHARM code can be found in Quackenbush et al. (1999) and references cited therein. The key enabling technologies of the model include: (a) curved vortex elements with an analytical solution for the self-induced velocity effect (Bliss et al., 1987a), (b) a full-span Constant Vorticity Contour (CVC) wake model that directly computes wake rollup (Bliss et al., 1987b), (c) inclusion of fast hierarchical vortex methods (Quackenbush et al., 1996, 1999), and (d) physics-based models of the internal core structure of the rolled up tip vortex (Wachspress and Quackenbush, 2001; Rule and Bliss, 1995, 1998).

CHARM delivers highly accurate solutions over a broad range of applications. It is designed in a hierarchical structure to enable a single code to apply to a wide range of modeling tasks. These tasks include the prediction of extremely high resolution airloads and flow fields, flight dynamic applications, including real-time aeromechanics solutions suitable for pilot training, engineering flight simulations, and qualities analyses. CHARM is the default helicopter model used by >35 helicopter manufacturers, government organizations, and foreign entities worldwide. Licensing of the executable code is also supported by Mount Rose Scientific, LLC. A summary of their basic inputs is given in Table 1 A comparison of the predicted wake decay for the ICON, PV22, and PV35X is shown in Fig. 1.

The combination of CHARM + AGDISPpro enables rapid deposition predictions that render the combined codes suitable for control of drift

Table 1
Summary of RPAAS models simulated by CHARM to date.

Name	Number of Rotors	Semispan (m)	Speeds (m s^{-1})
Aeronavics ICON	Octocopter (4 over 4)	0.890	2 to 12
Yamaha RMAX	Single Rotor (small helicopter)	1.558	2 to 12
DJI Agras MG-1	Octocopter (8 in one plane)	0.738	2 to 8
PV22	Quadcopter (4 in one plane)	0.964	1 to 5
PV35X	Hexacopter (6 in one plane)	1.202	1 to 5
DJI Agras T30	Hexacopter (6 in one plane)	1.429	2.3 to 7
Tiannong M6E-X	Hexacopter (6 in one plane)	0.946	0.6 to 4
Tiannong M8E Pro hexacopter	Hexacopter (6 in one plane)	1.131	2 to 6
PV40X	Hexacopter (6 in one plane)	1.473	1 to 10

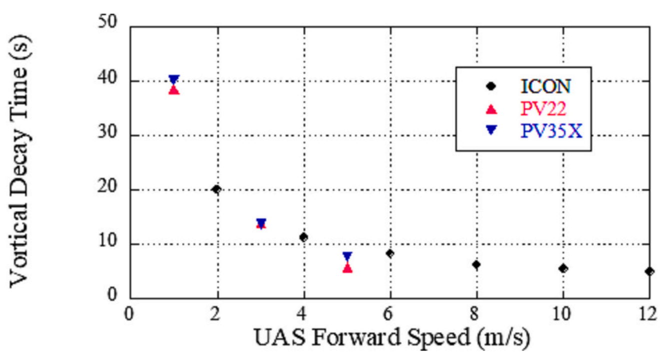

Fig. 1. Graphical representation of RPAAS vortical decay time as a function of forward speed, as interpreted from CHARM calculations that include decay times suggested by Donaldson and Bilanin (1975) and supported by an extensive set of aircraft anemometer tower grid flyovers (Teske et al., 1993a; Teske and Thistle, 2003).

during aerial applications. The inclusion of the aerial release of pesticides and the subsequent motion of the released spray material were first discussed in Teske et al. (2018b), though the version used here uses a pre-computed RPAAS flow field database generated with CHARM to reduce computational turnaround time.

Two RPAAS were used in this study: Leading Edge Aerial Technologies PV22 and PV35X. Their input characteristics are summarized in Table 2. Pictures of these RPASS on the field can be found in Figure SM2–4 (SupplementaryMaterials_Figures_SM2.docx).

Table 2
Characteristics and limits of RPAAS modeled in AGDISPpro for this study.

Characteristic	PV22 Quadcopter	PV35X Hexacopter
Spraying Speed (m s^{-1})	3.0	3.0
Weight (kg)	21.0	29.7
Boom Half Width (m)	0.964	1.202
Rotor RPM	2531.0	2483.0
Boom Vertical Position (m)	−0.51	−0.61
Boom Forward Position (m)	0.0	0.0
CHARM Data File Name	PV22.uav	PV35X.uav
X Reference Centerline (m)	CL of RPAAS	CL of RPAAS
Z Reference Centerline (m)	Height of Rotor Blades	Height of Rotor Blades
Speed Limits (m s^{-1})	1.0 to 5.0	1.0 to 5.0
Weight Limits (kg)	18.0 to 24.0	26.0 to 33.6
Height Limits (m)	1.0 to 10.0	1.0 to 10.0
Boom Vertical Limits (m)	−0.76 to −0.26	−0.86 to −0.36
Boom Forward Limits (m)	−0.576 to 0.576	−0.813 to 0.813

2.2. Field data collection

RPAAS operational, meteorologic, and agronomic data, as well as in-swath and off-target drift deposition samples were obtained from two field studies. These studies were specifically designed to quantify in-swath and off-target depositions from spray applications using commercially available RPAAS in realistic environmental and field conditions. No pesticide was used. Instead, fluorescent tracer dye was used as the spray material in both field trials. Both trials partially followed standard guidelines and/or recommended protocols for conducting spray drift trials (ISO, 2005) with variations to meet the purposes of each study. Variations included number of application events and type of reference spray platform.

The first experiment, herein referred to as study no. 1, was conducted at the West Central Research and Extension Center at the University of Nebraska–Lincoln, North Platte, Nebraska, USA on Oct 19 and 20, 2020. Study no. 1 is discussed in Martin et al. (2024).

The second experiment (study no. 2) was conducted on a private property in Shelbourne, Vermont, USA on November 2–4, 2021. Details of study no. 2 research are presented in Rice et al. (2022). Both sites are flat agricultural areas in open spaces unobstructed by tree lines or any other structures, making them suitable for spray drift studies (ISO, 2005).

Table 3 summarizes the main characteristics of the two field studies relevant to this research. The PV22 quadcopter was employed in study no. 1. The PV35X hexacopter, a larger RPAAS, was used in study no. 2. Both RPAAS are manufactured by Leading Edge Aerial Technologies (Leading Edge Aerial Technologies, 2023). The RPAAS used in study no. 2 had six nozzles on its spray boom whereas the RPAAS used in study no. 1 had four nozzles.

In study no. 1, nozzles representing two spray qualities were included: the TT110–01, which has an ASABE Medium droplet size distribution (DSD), and the TTI110–01, an air induction nozzle with an Extremely Coarse DSD. Both nozzles are manufactured by TeeJet. Each of these spray quality treatments was replicated 12 times. In study no. 1,

Table 3
Characteristics of RPAAS spray deposition field studies used for the AGDISPpro evaluations.

Parameter	Study No.	
	1	2
Location	Nebraska	Vermont
Ground Cover	Bare soil and crop residue	Grass turf (5 cm tall)
RPAAS Platform	PV22	PV35X
Number of Rotors on RPAAS	4	6
Number of Nozzles on RPAAS	4	6
Number of RPAAS Treatments	2	6
Number of Replicates per Treatment	12	1
Number of Application Passes	1	4
In Swath Deposition Collection Locations (m from edge of the field)	1 transect per replicate: 0 m to −7 m, every 0.5 m (n = 15)	See Table 5
Off-Target Deposition Collection Locations (m from edge of the field)	1 transect per replicate: 0.5 m to 10 m, every 0.5 m; 10 m to 50 m, every 5 m. 50 m to 100 m, every 10 m (n = 33)	3 transects per repetition: 0.5, 1, 2, 4, 8, 16, 32, 46 and 100 m (n = 27)
Target Test Dye	PTSA	Rhodamine WT 20 %
Nozzle spacing (from center line in the spray boom, in m)	−1.14, −0.381, −0.381 and 1.14	see Table 5
Target application rate (g ha^{-1})	18.7	280

applications using a ground boom were also performed using comparable spray qualities (ISO, 2005); These application events were out of the scope of this research and therefore not considered. Flying velocities were 2.95 m s^{-1} and 4.4 m s^{-1} for the Medium DSD and Extremely Coarse DSD treatments, respectively. In both treatments, the spray release height was 3.04 m from the ground. Spray release height and speed were measured using the onboard GPS with Real Time Kinematics (RTK) correction, and with sub meter location precision. All application events consisted of single swath applications with a targeted spray width of 5 m for medium DSD nozzles and 3 m for extremely coarse DSD nozzles. The operational pressure during application events for both treatments in study no. 1 was 275.8 kPa.

In study no. 1, the spray flow rate was 6.3×10^{-2} L sec^{-1}. The dye used was PTSA (SPECTRA TRACE SH-P by Spectra Color Corporation) which is a soluble salt. The tank concentration was 1 g L^{-1}. In study no. 2, Rhodamine WT, 20 % dye was used. The field study spray volume application rate was set to 46.8 L ha^{-1}. The fraction of application rate was calculated in both studies based on the target application rate, area of the sampling media, and observed deposition rates for each sample.

Swath width specific to each application event was determined from post-application analysis of the spray drift deposition data collected during study no. 1 (Table 4). The process of reevaluating the spray swath widths and application rates followed several steps. Each application event deposition profile was evaluated following the procedures established by the ASABE standard for establishing effective swath widths (ASABE, 2012). This process is documented in Fritz and Martin (2020), but in summary, for each application event seven copies were mathematically spaced at increasing intervals (0.5 to 20 m in 0.5 m increments) to determine the contribution of adjacent swaths to the total progressive deposition pattern. The progressive overlap pattern was then analyzed for uniformity and application rate. While effective swath width is defined by the standard as the maximum swath that achieves a specified level of uniformity, commercial applications are required to meet application rates established by product labels. ASAE 327.4 JUL2012 (R2021) notes that criteria other than uniformity may be used when establishing an effective swath width. Recognizing that uniformity alone is not sufficient when evaluating RPAAS spray patterns, Fritz and Martin (2020) established the use of the effective application rate as a metric for selecting an appropriate effective swath width. Simply stated, the maximum swath width that achieves a specified application rate across the progressive overlapped pattern is selected as the effective swath width.

Table 4
Calculated swath widths and corresponding swath displacements (m) used in model simulations for study no. 1.

DSD	Application Event	Swath Width	Swath Displacement
Medium	1	2.7	1.2
	2	2.7	1.2
	3	3.1	1.0
	4	4.1	0.5
	5	3.1	1.0
	6	1.7	1.7
	7	3.0	1.0
	8	2.2	1.4
	9	2.9	1
	10	4.1	0.5
	11	3.4	0.8
	12	3.8	0.6
Extremely Coarse	13	1.7	1.6
	14	1.8	1.6
	15	1.5	1.8
	16	2.9	1.1
	17	2.0	1.5
	18	2.0	1.5
	19	2.1	1.5
	20	2.0	1.5
	21	2.0	1.5
	22	2.4	1.3
	23	2.6	1.2
	24	2.0	1.5

Applying these methods across all passes of both RPAAS application events using the targeted application rate of 18.7 L ha^{-1} resulted in swath widths that were narrower than those intended (Table 4). Prior to the field drift study, the setups used for the RPAAS treatments were tested to confirm intended swath width and application rate and did indeed indicate that the RPAAS medium DSD nozzle treatment achieved 18.7 L ha^{-1} with a 5 m swath spacing. The RPAAS coarse DSD nozzle treatment, however, required a narrower swath spacing of 3 m to meet the targeted rate. There were limited replications, and the spray passes were done with the RPAAS flying parallel to the wind direction, which is a common practice for these types of evaluations. RPAAS spray applications conducted under crosswind conditions were shown to produce highly variable and displaced distribution patterns that required reduced swath width to achieve intended application rates as compared to applications made parallel to the wind direction (Fritz and Martin, 2020).

Swath displacements required for AGDISPpro were determined using the calculated effective swath widths for all the RPAAS application events in study no. 1. In AGDISPpro, the edge of the application area is initially defined by swath offset. The default swath offset in the model assumes that the RPAAS is upwind of the edge of the application area by one-half swath. Swath displacement in AGDISPpro allows the user to offset the flight line an additional distance to account for wind effects. For study no. 1, the swath displacement for each i^{th} application event was calculated as 2.5 – (1/2*swath width). 2.5 (in m) representing the distance from the flight centerline to the reference edge of the field established in study no. 1 (Table 4).

In study no. 2, six application events were conducted to compare spray drift under various conditions of spray quality, nozzle spacing, and spray release height (Table 5). The two nozzles compared were the TTI 11003, producing an Ultra Coarse DSD and the XR 11003, producing a Fine DSD. Both nozzles are manufactured by TeeJet. The two nozzle spacings compared consisted of a “compact” configuration where the third pair of nozzles was placed 1.24 m from the spray boom's center and an “outside” configuration where the third pair of nozzles was at 1.3 m from the center of the spray boom. The two spray release heights tested were 2 and 3 m above ground. Each treatment was conducted once without replication. In all application events, multiple swaths were sprayed with a targeted swath width of 4.88 m. This swath width was determined by the RPAAS pilot after reviewing spray pattern testing results. The RPAAS flew at an application velocity of 4.4 m s^{-1} for all applications. Both spray release height and speed were measured using the onboard GPS with Real Time Kinematics (RTK) correction, with one-centimeter relative location precision. The operating pressure during spray applications in study no. 2 was 349.6 kPa psi.

In both field studies, Mylar cards, a commonly used sampler, were used to collect in-swath and drift deposition samples. Fluorimetry techniques were used to measure the mass of dye found in each deposition sample. A Turner Designs Trilogy® Laboratory Fluorometer was used. These devices were fitted with a PTSA and a Rhodamine and Phycoerythrin modules for studies no. 1 and no. 2, respectively. In study no. 1, one deposition sample was collected in each of the 15 in-swath distances, and in each of the 33 off-target spray downwind distances per application event (Table 3). A schema with the locations of horizontal deposition sample collectors in relation to the edge of the field can be found in Figure SM2–5 in the document titled SupplementaryMaterials_Figures_SM2.docx. In study no. 2, 27 off-target spray deposition samples were collected per application event, representing 9 downwind distances. Off-target spray samplers were organized in three parallel transects. The number of in-swath samples ranged from a minimum of 6 to a maximum of 18 in this study across the different application events (Table 5). A schema with the locations of horizontal deposition sample collectors in relation to the edge of the field can be found in Figure SM2–5 in the document titled

Table 5
Characterization of study no. 2.

Nozzle DSD	Application Event	Nozzle Configuration	Release Height (m)	Nozzle Spacing (m)	In-Swath Sample Spacing	No. of In-swath Samples Collected	Average Representative In-swath Fraction of Applied
Ultra Coarse	1	Compact	2	From center line: 0.25, 0.76, 1.24	Three samples at 0 m from edge of the field. Individual samples at −4.3 m, −9.1 m, −14 m and − 18.9 m	7	0.55
	3	Compact	3	From center line: 0.25, 0.76, 1.24	Three samples at 0 m from edge of the field. Individual samples at −4.3 m, −9.1 m, −14 m and − 18.9 m	7	0.74
	4	Outside	3	From center line: 0.25, 0.76, 1.3	Three samples at 0 m from edge of the field. Individual samples at −4.3 m, −9.1 m, and − 14 m	6	0.80
Fine	5	Compact	2	From center line: 0.25, 0.76, 1.24	Three samples at 0 m from edge of the field. Individual samples at −4.3 m, −9.1 m, and − 14 m. Two samples at − 18.9 m	8	0.60
	7	Compact	3	From center line: 0.25, 0.76, 1.24	Three samples at 0 m from edge of the field. Individual samples at −0.6 m, −1.8 m, −4.3 m, −5.5 m, −6.7 m, −7.9 m, −9.1 m, −10.4 m, −11.6 m, −12.8 m, −14 m, −15.2 m, −16.5 m, −17.7 m and − 18.9 m	18	1.00
	8	Outside	3	From center line: 0.25, 0.76, 1.3	Three samples at 0 m from edge of the field. Individual samples at −0.6 m, −1.8 m, −3 m, −4.3 m, −5.5 m, −6.7 m, −7.9 m, −9.1 m, −10.4 m, −11.6 m, −12.8 m, −14 m, −15.2 m, −16.5 m, −17.7 m and − 18.9 m	19	1.00

SupplementaryMaterials_Figures_SM2.docx. In general, both studies followed the minimal standard procedure for sampling spray drift deposition, both in-swath and off-target (ISO, 2005).

In both studies, weather data were collected for wind speed, wind direction, surface air temperature, and relative humidity. In study no. 1, a meteorological monitoring station equipped with a Met One instrument was employed (Martin et al., 2024). This station included instruments to capture wind speed (Model 010C, accuracy of ±3 %), wind direction (Model 020C, accuracy of ±3 %; North = 0°), and temperature and relative humidity (Model 085, accuracy of ±0.15C° and ± 2 % respectively). The meteorological data were collected every second at 2 m above the ground and approximately 20 m downwind of the 100 m sampling transect. Summary statistics of the meteorological data collected during all application events of study no. 1 are provided in Table SM1–1, in the Supplementary Materials document titled “SupplementaryMaterial_Tables_SM1.docx”. The averages of the wind direction relative to the RPAAS flight path, temperature, and relative humidity calculated from all individual application events were − 105.1°, 12.9C°, and 49.6 %, respectively. The average wind speed across all application events was 3.5 m s^{-1}, with a range from 1.9 m s^{-1} to 5.8 m s^{-1}. In application events 4, 16, 17 and 18, wind deviation was >120°. Although spray drift study standards specify that wind direction relative to the flight path should not be outside the −90 ± 30° range (ISO, 22866, 2005), we included these events for modeling purposes. The lowest wind speed was 1.6 m s^{-1} and in application events 8, 9, 18, and 19, wind speed exceeded 5 m s^{-1}.

For study no. 2, the meteorological monitoring station was equipped with a Gill Instruments' Windsonic device that measures wind direction and speed and a Campbell Scientific CS215 instrument to collect temperature and relative humidity data. These instruments provide an accuracy of ±2 %, 2 %, ± 0.4 °C, and ± 2 % for wind speed, wind direction, temperature, and relative humidity, respectively. All measurements were collected 2 m above the ground with a temporal resolution of 1 s. Table SM1–2 (SupplementalMaterial_Tables_SM1.docx) provides summary statistics of the meteorological parameters collected in all application events. The average values of the wind direction relative to the RPAAS flight path, temperature, and relative humidity calculated from all individual application events were: −81°, 5.1 °C, and 78.1 % respectively. The average wind speed across all application events was 1.8 m s^{-1}, with a range from 1.3 m s^{-1} to 2.3 m s^{-1}. During application event 5, the wind direction relative to the fly path was −45°, which is higher than the standard −90 ± 30° range (ISO, 22866, 2005). This event was included in the modeling.

2.3. Modeling approach

AGDISPpro version 0.6 was used for modeling spray deposition from the selected RPAAS field studies. Specific flow field models were developed for the RPAAS employed in the field spray applications. To parametrize model runs in AGDISPpro, data from the field records acquired in studies no. 1 and 2 describing the RPAAS flight and application, spray material, and meteorological environment were used. The required RPAAS flight and application information included aircraft type and description, spray release height, flight speed, spray swath displacement, spray nozzle configuration, droplet size spectra (referred to as nominal DSD in AGDISPpro), and swath width. Spray material information included fractions of the tank mix classified as the carrier, the active, and the additive components of the mixture, as well as the spray volume rate. Meteorological information included wind speed and direction, temperature, and relative humidity for each spray pass (Table S1 and Table S2). 24 AGDISPpro simulations were parametrized and modeled using information obtained from each application event performed in studies no. 1. In study no. 2, six simulations were parametrized and modeled using data collected from the respective field application events. Table 6 summarizes the parameters used when parameterizing all model runs included in the analysis. The AGDISPpro

Table 6
Input parameters from studies no. 1 and 2 used for AGDISPpro simulations.

Group	Parameter	Study No.	
		1	2
Application method	Flow field model file name	PV22	PV35X
	Typical flight speed (m s^{-1})	Medium DSD: 2.68; Extremely Coarse DSD: 4.43	4.38
	Release height (m)	3.05	See Table 5
	Spray lines	1	4
Application technique	Number of nozzles	4	6
	Nozzle spacing (m)	1.14–0.381	See Table 5
	DSD	Custom Medium (DV_{50} 210 μm at 40 psi) and Extremely Coarse (DV_{50} 587.9 μm at 40 psi)[a]	ASABE Fine and ASABE Ultra Coarse
	Swath width (m)	See Table 4	4.88
	Swath displacement (m)	See Table 4	0
Meteorology	Wind speed, wind direction, temperature, relative humidity	See **Table S1** supplemental materials	See **Table S2** supplemental materials
Spray material[b]	Spray material evaporates	Yes	Yes
	Spray volume rate (L ha^{-1})	22.21	46.76
	Nonvolatile active fraction	0.001	0.0012
	Nonvolatile fraction	0.001	0.0012
	Fraction of active solution that is nonvolatile	1	1
	Additive fraction of tank mix	0	0
	Fraction of additive solution that is nonvolatile	1	1
Atmospheric stability	Atmospheric stability	Moderate	Moderate
Surface	Upslope angle (deg)	0	0
	Sideslope angle (deg)	0	0
Canopy	Type	None	non
	Surface roughness	0.0075	0.0075
Advanced settings	Wind speed height (m)	2	2
	Default swath offset	1/2 swath	1/2 swath
	Specific gravity (active/additive)	1.6	1.8

[a] . Specific droplet diameter distribution tables were made available for both nozzles by the manufacturer, and these were included in AGDISPpro as a custom class. The reported DV_{50} value for the TeeJet TT110–01 nozzle does not correspond to the standard ASABE Medium DSD class DV_{50} value, however the manufacturer classifies this nozzle as such.

[b] . In the spray material parameters, values are provided as fraction of the tank mix volume.

model parametrization section in the supplemental materials provides additional explanation of how the field data were processed and summarized for model setup.

2.4. Model evaluation

To assess the accuracy of the predictions produced with AGDISPpro, model results were compared to field deposition measurements.

AGDISPpro generates predictions every 2 m from the most upwind in-swath position to the most downwind position of the spray deposition plume. Predictions were linearly interpolated to the exact location where field samples were collected in those cases where distance to the edge of the field in the model did not exactly match field observation locations In study no. 2, three replicates were collected at every off-target spray drift sampling distance (see Table 3 and fig. SM2–5 in SupplementaryMaterials_Figures_SM2.docx). Therefore, field-collected deposition samples were averaged at every off-target sampling distance.

Using the set of matched predicted and observed data values, model evaluation statistics were calculated both on a per application event basis and across all application events for a given nozzle. These statistics were: the index of agreement (10) and mean bias error (11):

$$r\ index = 1 - \frac{\sum (P_i - O_i)^2}{\sum (|P_i - O| + |O_i - O|)^2} \tag{10}$$

$$d = \frac{\sum (P_i - O_i)}{n} \tag{11}$$

In these equations, O_i and P_i are the observed and predicted values, respectively, for each i^{th} sample; O is the mean value of O_i for each repetition i and n is the number of observations per repetition.

The index of agreement varies from 0 to 1 with higher index values indicating that the modeled values P_i have better agreement with the observations, O_i. A value of 1 indicates a perfect match and 0 indicates no agreement at all (Willmott, 1981). In the case of d, this statistic was used to assess whether the model was under predicting (a negative value) or overpredicting (a positive value). These model performance metrics are described in Duan et al. (1992), where they were used in an evaluation of an early version of the AGDISP model. Furthermore, we included the R^2 of Ordinary Least Square (OLS) regressions comparing model predictions and field observations. All calculations were performed using the "Base" and "Stat" packages in R (R Core Team, 2022). Residuals of the linear models fitted to the data were evaluated to confirm assumptions about normality and heteroscedasticity. We calculated goodness-of-fit statistics for the complete set of in-field and off-target measurements for each application event, and the subset of off-target drift measurements. Finally, we compared the area under the off-target drift deposition curves calculated from the field measurements and the model simulations using the "AUC" (Area Under Curve) function in the DescTools R package with the "spline" method. The percent difference between model prediction and field measurement for each application event was calculated based on AUC output. A one sample t-test was used to evaluate if the percent difference in AUC across each DSD type was statistically different between the measured and modeled total drift deposition. Input AUC values in the analysis followed a normal distribution.

In study no. 2, fraction of applied values obtained from field observations were adjusted to account for insufficient field data. Swath width provided in field observations was the same for all application events. However, swath width should vary given the spray volume rate and differences between nozzle DSDs and release heights. Unfortunately, with the available information, it is impossible to calculate specific swath widths and target application rates for all application events. To partially account for this data gap, fraction of applied values obtained from field observations were adjusted in the following way. First, a representative average in swath fraction of applied value was calculated for each trial run in study no. 2 (Table 5) using the available in-swath field data collected below or near the flight path of the RPAAS. These values were used to normalize the fraction of applied values of all samples using the following formula:

$$Normalized\ fraction\ of\ applied_{i,j} = \frac{fraction\ of\ applied_{i,j}}{\text{average in swath fraction of applied}_j} \tag{12}$$

In this formula, the i^{th} and j^{th} index refers to the distance and field application event, respectively.

2.5. Sensitivity of predicted deposition to swath width and swath displacement

Determining swath width and swath displacement in RPAAS applications is challenging and efforts to establish the best methodology are being researched. Typical pattern testing in a spray drift field study estimates swath width with RPAAS flying into the wind. However, the design of spray drift studies requires RPAAS flying across wind. Clearly, this inconsistency causes uncertainty in swath width and the corresponding swath displacement estimates. To understand the effect of varying swath width and swath displacement assumptions on spray drift deposition patterns modeled in AGDISPpro, we conducted a sensitivity analysis in which we modified these two parameters while holding all other conditions constant for application event 1 (Medium DSD) and application event 13 (Extremely Coarse DSD) from Study no. 1. Swath widths ranging from 1 to 5 m with 0.5 m increments being tested ($n = 9$). For each swath width value, swath displacement was then calculated as 2.5 m minus one half the swath width.

3. Results and discussion

3.1. Study no. 1

Fig. 2 (log10 scale) and Figure SM2–1 (linear scale, in the SupplementaryMaterials_Figures_SM2 document) compare the field observations and AGDISPpro predictions of spray deposition for individual application events in the Medium DSD treatment in study no. 1.

To evaluate model performance, robust field data are needed. For the Medium DSD treatment in study no. 1, the maximum deposition (peak) occurred at distances >3.5 m downwind from the edge of the field in application events 2, 8, and 9. Thus, the central mass of the disposition shifted well-away from the applied area during these application events. This central deposition mass shift for these three events was inconsistent with other application events under similar conditions. Although the post-processing process described in Section 2.2 was intended to mitigate the issue by deriving event specific swath width and the corresponding swath displacement, the dislocation of central mass is still not fully addressed for those three application events. Given these abnormalities and uncertainty regarding the cause, the modeling results from these three applications events are presented graphically, but they are excluded from the summary statistics and discussion.

Fig. 2 and Figure SM2–1 (SupplementaryMaterials_Figures_SM2 document) indicate that model predictions of maximum deposition (peak) in each application event generally compared well with observed values. However, maximum deposition (peak) in the modeled predictions were generally biased to varying degrees upwind of the edge of the field compared to the observed values. In several application events, maximum deposition was shown in the off-target drift section of the spray plume. This result indicates that despite the curves produced from the field samples and AGDISPpro predictions being similar in shape and magnitude, their displacement relative to the intended edge-of-field location can be inconsistent.

In seven out of 12 simulations, modeled results correspond well with the observed spray drift deposition around the peak fraction of applied and nearby samples immediately up and downwind (Fig. 2). Model simulations tended to underpredict deposition in the further downwind off-target distances for the Medium DSD application events.

The results of the statistical evaluation of model simulations compared to observed deposition for the Medium DSD application events are provided in Table 7. For the combined in-field and off-target

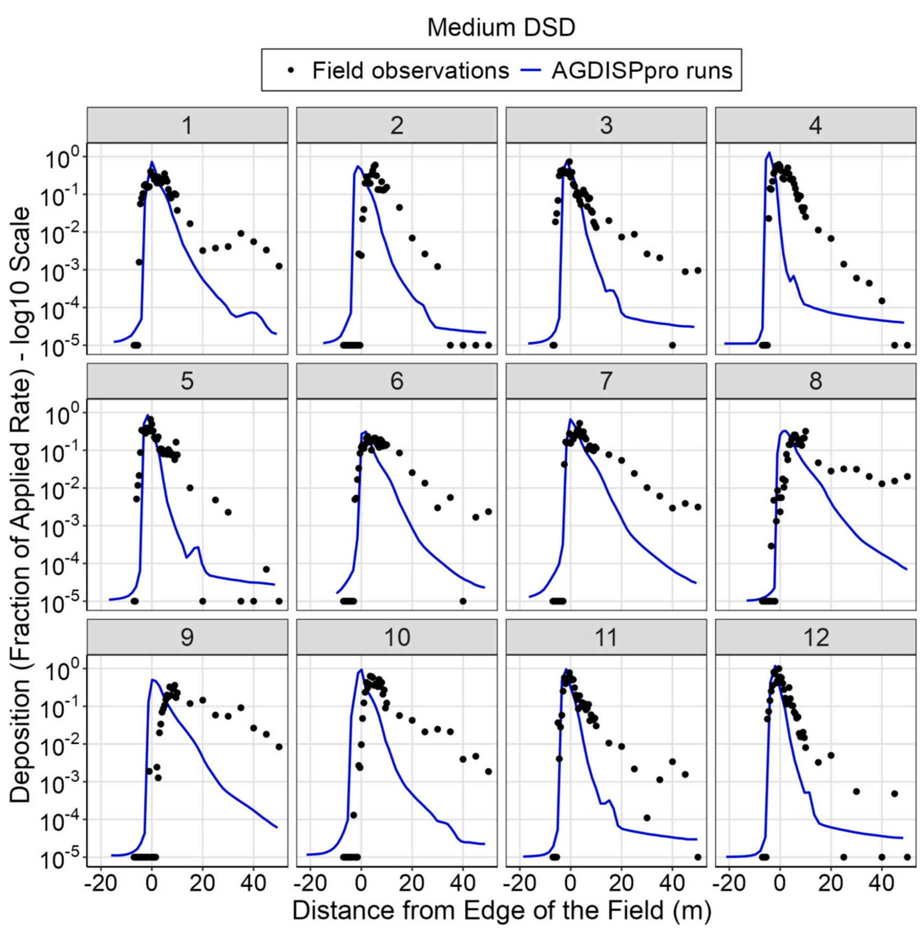

Fig. 2. AGDISPpro deposition predictions versus field measurements (y-axis in log10 scale), medium DSD application events, study no. 1.

Table 7
Summary statistics comparing AgDISPpro modeled and field measured fraction of applied values, medium DSD application events, study no. 1[a].

Application Event	Location					
	In-Field Deposition & Off-Target Drift			Off-Target Drift		
	r index	*d*	R^2	r index	*d*	R^2
1	0.81	−0.002	0.58*	0.81	−0.023	0.53*
3	0.89	−0.004	0.68*	0.92	−0.014	0.79*
4	0.24	0.004	0.02	0.47	−0.148	0.40*
5	0.85	−0.005	0.64*	0.83	−0.051	0.82*
6	0.78	−0.012	0.39*	0.70	−0.027	0.27*
7	0.75	0.012	0.42*	0.77	−0.019	0.31*
10	0.27	0.021	0.01	0.49	−0.121	0.002
11	0.84	−0.001	0.54*	0.79	−0.068	0.92*
12	0.86	0.002	0.58*	0.72	−0.070	0.89*
Median of Events	0.81	−0.001	0.54*	0.77	−0.051	0.53*
All Events Pooled Together	0.67	−0.003	0.31*	0.68	−0.043	0.38*

[a] : Abbreviations of model fit indicators are r index = index of agreement and d = mean bias error.
* *p*-value≤0.05.

drift deposition in the Medium DSD application events, the r index ranged from 0.24 to 0.89, with a median of 0.81. In seven out of nine simulations, the index of agreement was above 0.7, indicating good agreement between field measurements and model predictions. The mean bias error (*d*) ranged from −0.012 to 0.021, with a median of −0.001, with five of nine application events having negative values. R^2 values ranged from 0.01 to 0.68, with a median of 0.54. In five out of nine application events, R^2 values of the modeled and measured deposition data were above 0.5. When pooling all application events together, the r index, *d*, and R^2 were 0.67, −0.003, and 0.31, respectively. The modestly lower statistics for the pooled events compared to the median indicate that a few poorly performing events (i.e., events 4, and 10) skewed the pooled statistics.

The goodness-of-fit statistics for the off-target drift deposition indicate a similar level of agreement to the statistics for the complete in-field and off-target deposition data (Table 7). Residuals in all the linear regressions performed for the statistical comparison of modeled and predicted values in study no. 1 followed a normal distribution. The r index ranged from 0.47 to 0.92, with a median of 0.77. In seven of nine cases, the r Index was above 0.7, indicating a good model representation of the field observations. Mean bias error (*d*) estimates for off-target drift deposition ranged from −0.148 to −0.014, with a median value of −0.051, indicating the model underpredicted spray drift deposition for all nine of the application events. R^2 values ranged from 0.002 to 0.92, with a median of 0.53. The R^2 values were above 0.5 in five of the nine application events considered, indicative of a good model fit. When pooling all application events together, the r index, *d*, and R^2 were 0.68, −0.004, and 0.38, respectively. Like the in-field and off-target drift statistics, a few poorly simulated events skewed these statistics downward, though the off-field drift statistics were slightly better. The average percent difference of the AUCs between AGDISPpro simulations and field measurements was −55.1 % with a 95 % confidence interval of −73.6 % to −36.6 % (t-value = −6.88, *p*-value <0.001). This *t*-test indicates that the AGDISPpro simulated AUCs, representing total drift deposition, are statistically different (lower, alpha = 95 %) than the

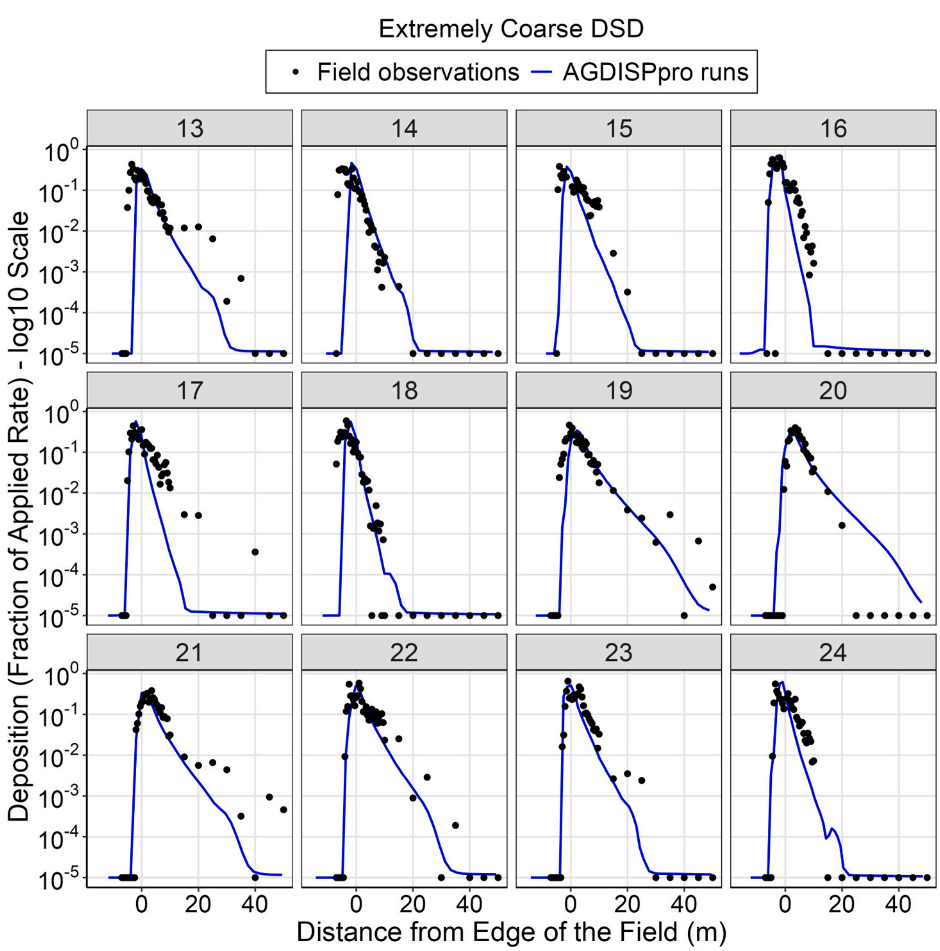

Fig. 3. AGDISPpro deposition predictions versus field measurements extremely coarse DSD application events, study no. 1.

AUCs calculated from the field data, and further indicates that the off-target drift deposition is under-predicted by the model.

The Extremely Coarse DSD simulations from study no. 1 show good correspondence between deposition peaks predicted by AGDISPpro and field observations, both in their magnitude and horizontal position (Fig. 3 in log10 scale and Figure SM2–2 in linear scale. In eight of the 12 simulations, peaks observed in the field slightly exceeded those predicted by AGDISPpro. For these application events, AGDISPpro predictions and field observed deposition results had very similar curves, both in magnitude and shape. Figs. 2 and 3 show that AGDISPpro performs better when simulating extremely coarse DSD applications than Medium DSD applications.

For the combined in-field and off-target drift deposition from the Extremely Coarse DSD simulations, the r index ranged from 0.59 to 0.94 (Table 8), with a median of 0.83. Ten of 12 simulations had r index values above 0.7, indicating good agreement between modeled and measured deposition. Values of *d* ranged from −0.035 to −0.002, with a median of −0.01, suggesting that AGDISPpro simulations under-predicted deposition compared to the measured across all application events. R^2 values ranged from 0.1 to 0.81, with a median of 0.49, and six out of 12 application events having values of 0.5 or greater, indicative of good model agreement. When pooling all application events together, the r index, *d*, and R^2 were 0.82, −0.010, and 0.47, respectively, similar to the median of the individual events. Residuals of all the linear regressions performed for the statistical comparison of modeled and predicted values followed a normal distribution.

The goodness-of-fit statistics for the off-target drift only deposition predictions were better than for the combined in-field and off-target drift deposition for the Extremely Coarse DSD simulations. When evaluating only the off-target drift modeled results, r index values ranged between 0.61 and 0.94, with a median of 0.88. In 11 of 12 simulations, r index values were above 0.7, indicating good model agreement. Values of *d* ranged from −0.041 to 0.021, with a median of −0.019, with negative values for eight of 12 application events. These results indicate that AGDISPpro underpredicted off-target spray drift deposition for the Extremely Coarse DSD applications. In this off-target drift subset of the data, R^2 values ranged from 0.43 to 0.95, with a median of 0.73. In 10 of 12 simulations, R^2 was above 0.5. When pooling all application events together, the r index, *d*, and R^2 were 0.89, −0.014, and 0.65, respectively, indicating a similar level of model performance as the median of the individual events. The average percent difference of the AUCs between AGDISPpro simulations and field measurements was −16.12 with a 95 % confidence interval of −48.8 % to 16.4 % (t-value = −1.09, *p*-value =0.3). This *t*-test indicates that the total off-target drift deposition predicted by AGDISPpro was not statistically different from those measured in the field, indicating the model is capable of predicting field drift measurements.

In study no. 1, AGDISPpro predictions for the Extremely Coarse DSD nozzle simulations were closer to the observations than the results from the Medium DSD nozzle simulations. In addition, the negative bias in the off-target drift deposition, as measured by the AUC statistics, was considerably smaller for the Extremely Coarse DSD nozzle applications. However, on an individual run basis within the Medium DSD application events, a reasonably good fit was observed in some model runs, such as application events no. 3 and 5. There are several reasons that could explain the better performance of AGDISPpro for extremely coarse DSD nozzles. First, it is possible that the swath width adjustment approach used in correcting dislocation of deposition central mass to off-field is more effective for larger droplets. Second, the heavier extremely coarse droplets are possibly less sensitive to the small-scale airflow complexities produced by the RPAAS and flight conditions in study no. 1 than the lighter medium-sized droplets. Additional research is needed to further understand and explain the performance difference of AGDSPpro predictions due to different spray qualities.

Table 8
Summary statistics comparing AgDISPpro modeled and field measured fraction of applied values, extremely coarse DSD application events, study no. 1[a].

Application Event	Location					
	In-Field Deposition & Off-Target Drift			Off-Target Drift Data		
	r index	*d*	R^2	r index	*d*	R^2
13	0.75	−0.012	0.32*	0.90	0.019	0.91*
14	0.59	−0.005	0.10*	0.85	0.021	0.92*
15	0.70	−0.035	0.27*	0.78	−0.019	0.46*
16	0.89	−0.004	0.65*	0.61	−0.032	0.60*
17	0.87	−0.010	0.64*	0.72	−0.034	0.67*
18	0.75	−0.002	0.35*	0.93	0.003	0.95*
19	0.82	−0.016	0.48*	0.92	0.019	0.72*
20	0.94	−0.007	0.81*	0.93	−0.019	0.77*
21	0.92	−0.010	0.73*	0.92	−0.029	0.72*
22	0.84	−0.012	0.52*	0.94	−0.008	0.75*
23	0.83	−0.004	0.50*	0.78	−0.044	0.43*
24	0.69	−0.012	0.29*	0.80	−0.042	0.73*
Median of Events	0.83	−0.010	0.49*	0.88	−0.019	0.73*
All Events Pooled Together	0.82	−0.010	0.47*	0.89	−0.014	0.65*

[a] : Abbreviations of model fit indicators are r index = index of agreement and d = mean bias error.
* *p*-value≤0.05.

3.2. Study no. 2

Model predicted peak deposition shows reasonable agreement with observed values for the ultra coarse DSD nozzle simulations (Fig. 4, in log10 scale and Fig. S3–3 in linear scale, found in SupplementaryMaterials_Figures_SM2.docx), both in magnitude and horizontal position. For the fine DSD nozzle simulations, AGDISPpro tended to underpredict the magnitude of the peak for in-field deposition, though the horizontal position was simulated well. In the Ultra Coarse DSD nozzle simulations, modeled off-field deposition values were generally lower than the observations. For two out of the three fine DSD nozzle model simulations, simulated deposition values had excellent agreement with the field data (application events 7 and 8).

The goodness-of-fit statistics for study no 2 are provided in Table 9. Residuals of all linear regressions performed for the statistical comparison of modeled and predicted values followed a normal distribution. For the ultra coarse DSD applications for the combined in-field deposition and off-target drift, r index values ranged from 0.34 to 0.86, with a median value of 0.74 (*n* = 3). In two of three simulations, the r index was above 0.7, indicative of good model fits. The mean bias error (*d*) ranged from −0.28 to −0.06, with a median of −0.20, indicative of general model underprediction. The R^2 values for simulations using the ultra coarse DSD nozzles ranged from 0.01 to 0.67, with a median of 0.44. One simulation resulted in an R^2 value higher than 0.5 (n = 3). When pooling all application events together, the r index, *d*, and R^2 were 0.60, −0.177, and 0.48, respectively, indicating a similar level of performance to the median of the individual events. The median statistics are limited by the small sample size.

For the off-target drift data only for the ultra coarse DSD application events, the goodness-of-fit statistics are slightly weaker than for the combined in-field and drift deposition. The r index values ranged from 0.48 to 0.55, with a median of 0.51 (n = 3). These results indicate moderate agreement between the measured and modeled off-target deposition. For off-target drift samples only, *d* values ranged from −0.5 to −0.28, with a median of −0.26, indicative of general model underprediction. For the off-target drift only, R^2 values ranged from 0.58 to 0.90, with a median of 0.89 (n = 3). When pooling all application events together, the r index, *d*, and R^2 were 0.48, −0.35, and 0.32, respectively. These pooled statistics indicate weaker model agreement for the off-target drift only predictions than the in-field and off-target combined predictions. The average percent difference in AUCs

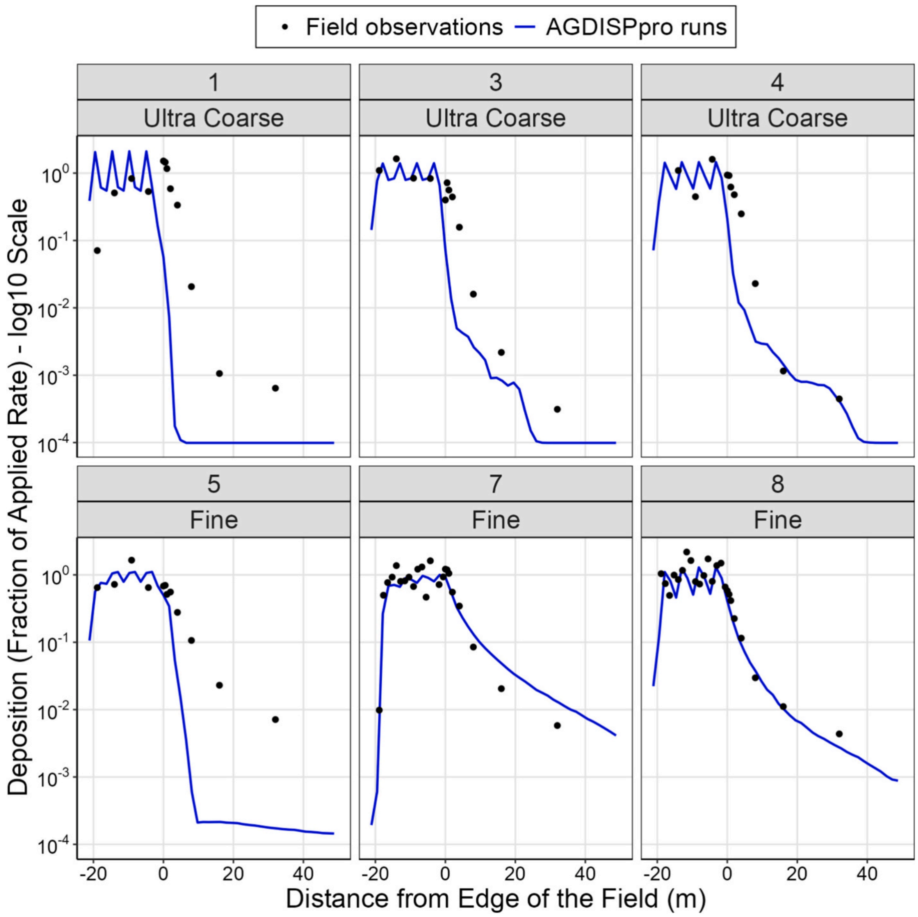

Fig. 4. AGDISPpro deposition predictions versus field collected data, study no. 2.

Table 9
Summary statistics comparing AgDISPpro modeled and field measured fraction of applied values, study no. 2[a].

DSD	Application Event	Location					
		In-Field Deposition & Off-Target Drift			Off-Target Drift		
		r index	*d*	R^2	r index	*d*	R^2
Ultra Coarse	1	0.34	−0.06	0.01	0.48	−0.50	0.90*
	3	0.86	−0.20	0.67*	0.51	−0.26	0.58*
	4	0.74	−0.28	0.44*	0.55	−0.28	0.89*
	Median of Events	0.74	−0.20	0.44	0.51	−0.26	0.89
	All Events Pooled Together	0.60	−0.177	0.48*	0.48	−0.35	0.32*
Fine	5	0.88	−0.08	0.65*	0.86	−0.14	0.91*
	7	0.84	−0.13	0.64*	0.93	−0.11	0.98 *
	8	0.76	−0.18	0.45*	0.93	−0.05	0.99 *
	Median of Events	0.84	−0.13	0.64*	0.93	−0.11	0.98*
	All Events Pooled Together	0.81	−0.14	0.54*	0.92	−0.10	0.95*

[a] : Abbreviations of model fit indicators are: r index = index of agreement and *d* = mean bias error.
* p-value ≤ 0.05.

between AGDISPpro simulations and field measurements was −94.1 with a 95 % confidence interval of −106.2 % to −81.9 % (t-value = −33.4, *p*-value <0.001). These *t*-test results suggest that the total off-target deposition obtained from the ultra coarse DSD application simulations were significantly lower than those measured in the field.

The AGDISPpro model simulations showed better agreement with field data for the application events using the Fine DSD nozzles for study no. 2. for combined in-field and off-target deposition, the r index values ranged from 0.76 to 0.88, with a median of 0.84 (n = 3), indicating good model agreement with field measurements for all application events. The *d* values ranged from −0.18 to −0.08, with a median of −0.13 (n = 3), indicating general underprediction by the model. The R^2 values ranged from 0.45 to 0.65, with a median of 0.64 (n = 3). When pooling the application events together, the r index, *d*, and R^2 were 0.81, −0.14, and 0.54, respectively, indicating slightly weaker model performance compared to the median event.

For off-target spray drift only with the fine DSD nozzle applications, the r index values ranged from 0.86 to 0.93, with a median of 0.93, indicating a good correspondence between modeled and measured deposition for all events. The *d* values ranged from −0.14 to −0.04, with a median of −0.11, indicating that the model tended to under predict drift deposition. The R^2 values for off-target drift were high, ranging from 0.91 to 0.99, with a median of 0.98. When pooling the application events together, the r index, *d*, and R^2 were 0.92, −0.10, and 0.95, respectively. The average percent difference in AUCs between AGDISPpro simulations and field measurements was −34.4 with a 95 % confidence interval between −119.2 % to 50.5 % (t-value = −0.75, p-value = 0.49). The t-test results indicate that the total off-target deposition obtained from the Fine DSD AGDISPpro simulations was not significantly different than those measured in the field.

Overall, AGDISPpro simulations in study no. 2 produced good agreement with field measurements, particularly for the off-target drift simulations. Model simulations had slightly better agreement with field observations for simulations using the fine DSD nozzles compared to those using the ultra coarse DSD nozzles. However, good agreement was still observed in several model runs using the latter nozzles. Study no. 2 was a multi-swath application study (four swaths per application event). It is encouraging that AGDISPpro can simulate spray deposition for multi-swath applications with a similar level of performance to the single-swath application events in study no. 1.

An important aspect of the comparison conducted between field spray deposition and the model-simulated deposition is the differences between the sampling resolution of field observations and the model predictions, particularly for the in-swath sampling. In study no. 1, the in-swath spatial resolution sampling of 0.5 m was higher than the 2.0 m resolution of the AGDISPpro model. In study no. 2, the in-swath sampling interval was in the 4 to 5 m range, coarser than the 2.0 m model resolution. Given the observed spatial variability of deposition, model fit statistics can be negatively influenced by small horizonal shifts in the predicted deposition profile relative to the observed samples. This horizontal resolution discrepancy can partly explain the deviations between the AGDISPpro model and field observations. Future studies designed to evaluate RPAAS spray deposition should adopt the higher resolution sampling regime of study no. 1, both in-swath and near-field off-target areas. Furthermore, the impacts of model output resolution on the statistical evaluation of model performance should be further explored to determine an optimal output resolution to support an unbiased model performance assessment.

Several evaluations of AGDISPpro and its predecessor (AGDISP) exist. For example, Duan et al. (1992) modeled pesticide applications using a Cessna Ag Truck C188, a twin propeller, light-weight agricultural aircraft. Comparison of AGDISP predictions and field-collected deposition samples indicated r index values ranged from 0.44 to 0.94 across the 7 application events considered. Combining data from all runs together, the r index of the comparison was 0.86. Comparing AGDISP modeled and field collected spray deposition from applications using Lockheed C-130 Hercules airplane, R^2 ranged between 0.411 and 0.968 (Teske and Whitehouse, 2022). The work presented in this manuscript is the first study to evaluate AGDISPpro spray deposition predictions from RPAAS in a detailed manner. Results from the comparison of AGDISPpro predicted and field collected deposition fall within the ranges observed from previous aerial spray drift modeling for conventional aircrafts.

3.3. Sensitivity analysis of swath width and swath displacement

The difficulty of estimating spray swath width and swath displacement for RPAAS and the resulting impacts on mechanistic modeling of spay drift deposition prompted a sensitivity analysis with AGDISPpro

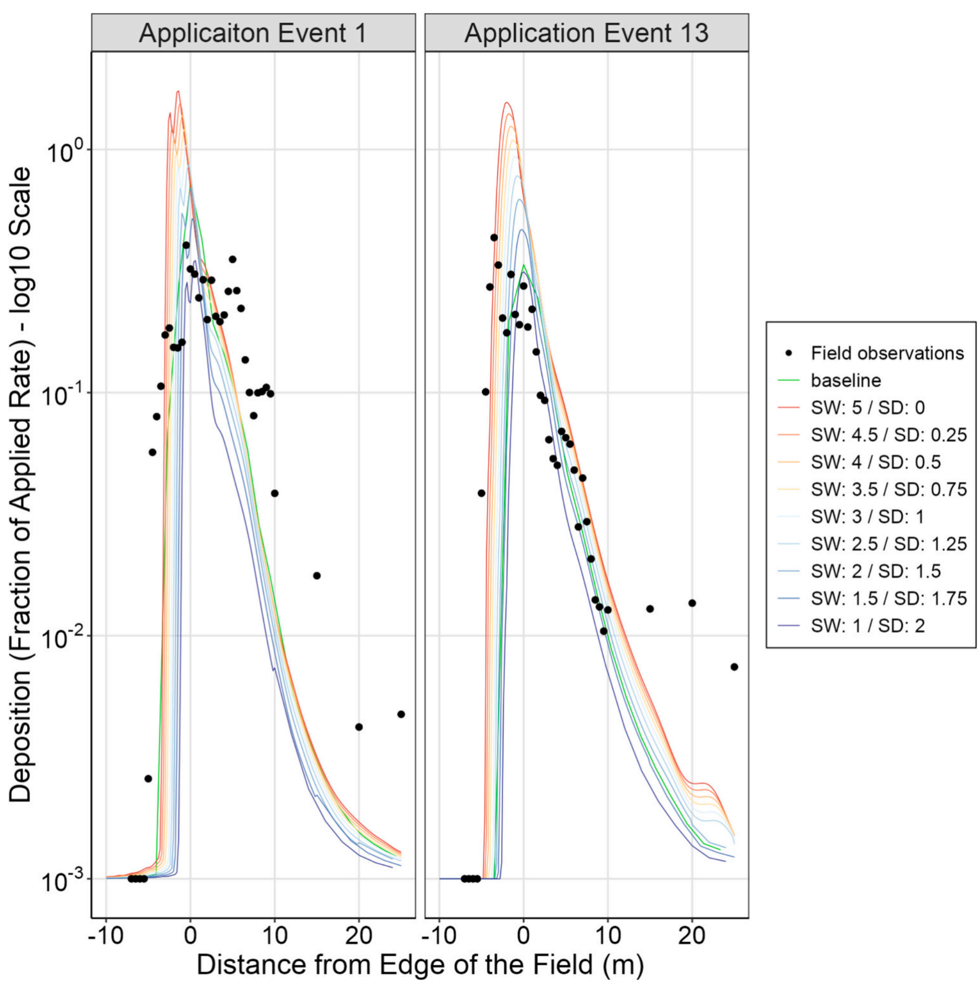

Fig. 5. Sensitivity of modeled deposition curves to changes in swath width (SW) and swath displacement (SD); baseline curve represents best initial estimates of SW and SD.

(described previously in Section 2.5). This analysis focused on two application events from study no. 1, one with medium DSD nozzles (event 1) and one with extremely coarse DSD nozzles (event 13). Fig. 5 presents the resulting deposition curves produced in the sensitivity analysis. The "baseline" simulations, symbolized in green, represent the AGDISPpro simulations using the best estimates of swath and displacement (Table 4). One very visible effect is a 3-to-5-fold increase in the magnitude of the deposition peaks. For application event 1, the baseline modeled peak was 0.73 fraction of applied, whereas in the ensemble of AGDISPpro simulations, peak deposition ranged from 0.35 to 1.74 fraction of applied. For application event 13, the baseline modeled peak was 0.33 fraction of applied, whereas in the ensemble of AGDISPpro simulations, peak deposition ranged from 0.31 to 1.56 fraction of applied. In addition, modifying the swath width and displacement has a moderate effect of extending the width of the deposition curve. However, the effect on displacement both upwind and downwind of the curve was limited to a few meters.

The effect of modifying swath width and displacement on goodness-of-fit statistics showed that the uncertainty in these parameters has an impact on the model's statistical performance. The r index of the off-target drift deposition was used to illustrate this impact (Fig. 6). In the simulations of event 1, the median r index calculated for the runs parametrized for the sensitivity analysis was slightly higher than the baseline r index value of 0.81 (Table 7). In five of nine simulations for the sensitivity analysis of event 1, the r index was higher than 0.81. For event 13, the median r index obtained from the sensitivity analysis simulations was 0.78, lower than the baseline r index for event 13 of 0.9 (Table 7). Only one of nine simulations from the sensitivity analysis resulted in a higher r index value than what was obtained from the baseline simulation.

This sensitivity analysis demonstrates the importance of accurate pattern testing to estimate swath width and displacement representing field study conditions. The analysis also indicates that the uncertainty of these parameters may be addressed in calibration of AGDISPpro simulations to achieve improvements of model performance. Physically-based models such as AGDISPpro often benefit from calibration of model parameters with field measurements to improve model performance. Uncertainties in other model inputs, such as specifics of the DSD, wind directio4n, and wind speed variation with height, also warrant consideration for calibration to improve model simulations of off-field drift deposition from RPAAS applications.

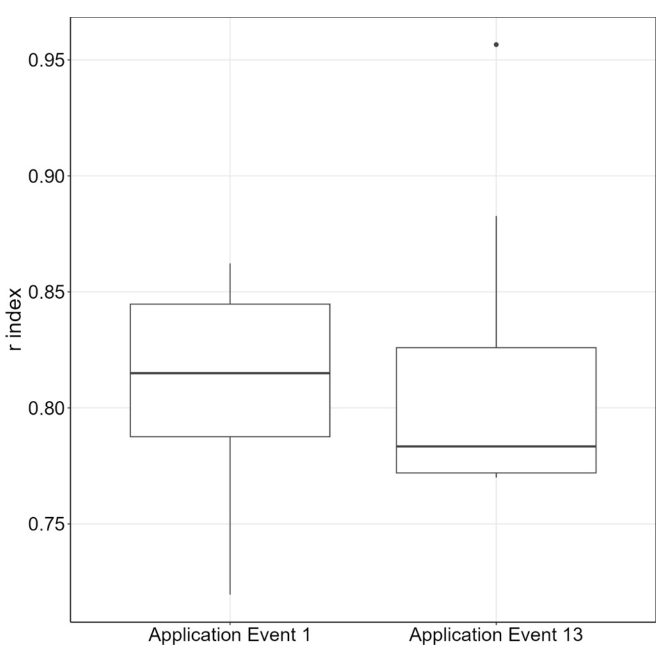

Fig. 6. Distribution of r index values from swath width/displacement sensitivity analysis (baseline simulations excluded).

The results obtained from this study demonstrate that AGDISPpro is a useful tool for modeling spray drift from RPAAS. Incorporating the AGDISPpro model into the regulatory framework of RPAAS is both promising and scientifically justified. As RPAAS and its associated spraying equipment continue to evolve, further validations of AGDISPpro on these platforms will strengthen the model's evaluation.

When planning research to further validate the utility of AGDISPpro for modeling spray drift from RPAAS, we suggest researchers should consider the following points. First, it is important to develop droplet size spectra specific to the equipment and conditions used during application events. This could be achieved by conducting wind tunnel experiments to determine droplet size spectra using the target equipment. For study no. 1, including specific DSD spectra provided by the nozzle manufacturer improved results compared to the standard ASABE DSD libraries contained in the software. For study no. 2, droplet size spectra (referred as nominal DSD in AGDISPpro) ASABE libraries found in the software were used. We would expect that the results would have been improved if explicitly measured droplet size spectra were available. Second, before conducting off-target spray drift deposition field studies designed to parametrize and evaluate AGDISPpro, it is important to accurately determine the expected swath width and swath displacement from RPAAS spray events. As demonstrated in section 3.3, swath width greatly impacts the shape and peak of the spray drift deposition curve. Incorporating realistic swath width and swath displacement values would likely improve the relative location of the modeled and observed spray drift deposition profile.

4. Conclusions

The use of RPAAS in the application of agricultural pesticides is increasing in many parts of the world and has the potential to greatly improve the efficiency and environmental sustainability of protecting our food supply. The need to evaluate the environmental and human health risks of pesticide use requires that the off-target movement and deposition of pesticide spray drift be quantified with a reasonable degree of certainty. The AGDISP model, which has a long history of use in quantifying off-target pesticide spray drift deposition from conventional fixed- and rotary-wing aircraft, has recently evolved to include the simulation of RPAAS. The research presented in this study provides the first validation of these recent AGDISPpro model enhancements through comparison with both single-swath and multi-swath RPAAS application field studies covering four different spray nozzle DSDs. This initial validation showed good agreement between the model simulated off-target drift deposition and the field observations for most application events, including both the single-swath and multi-swath studies. Some challenges were identified in both the practical application of RPAAS and their simulation with mechanistic models, namely the estimation of appropriate swath widths and displacement from these small aircraft. Both RPAAS design and their application technologies continue to evolve, with spatial uniformity of spray patterns one area of focus. Given the promising simulation results obtained in this study and the continued improvement in RPAAS spray technology, we anticipate that the ability of AGDISPpro and other models to accurately predict off-target spray drift deposition from RPAAS will continue to improve. Further research considering pesticide applications from additional RPAAS aircrafts with field studies designed explicitly for model validation should be conducted to more comprehensively validate AGDISPpro for use in regulatory decision-making.

CRediT authorship contribution statement

Sebastian Castro-Tanzi: Writing – review & editing, Writing – original draft, Visualization, Validation, Project administration, Methodology, Investigation, Formal analysis, Data curation, Conceptualization. **Michael Winchell:** Writing – review & editing, Writing – original draft, Validation, Supervision, Resources, Project administration, Methodology, Investigation, Funding acquisition, Formal analysis, Data curation, Conceptualization. **Zhenxu Tang:** Writing – review & editing, Writing – original draft, Validation, Supervision, Resources, Project administration, Methodology, Investigation, Funding acquisition, Formal analysis, Data curation, Conceptualization. **Milton E. Teske:** Writing – review & editing, Writing – original draft, Validation, Software, Methodology. **Glen R. Whitehouse:** Writing – review & editing, Writing – original draft, Validation, Software. **Brad Fritz:** Writing – review & editing, Writing – original draft, Validation, Methodology, Investigation, Formal analysis, Data curation. **Dan Martin:** Writing – review & editing, Validation, Methodology, Formal analysis, Data curation.

Declaration of competing interest

The authors declare the following financial interests/personal relationships which may be considered as potential competing interests: Sebastian Castro-Tanzi reports financial support was provided by Bayer Cropscience Ltd. Michael Winchel reports financial support was provided by Bayer CropScience Ltd. Glen R. Whitehouse reports financial support was provided by Bayer CropScience Ltd. Milton E. Teske reports financial support was provided by Bayer CropScience Ltd. Brad Fritz reports financial support was provided by Bayer CropScience Ltd. Dan Martin reports financial support was provided by Bayer CropScience Ltd. Zhenxu Tang reports financial support was provided by Bayer CropScience Ltd. co-authors have served as consultants to other projects funded by Bayer CropScience ltd; Glenn R. Whitehouse and Milton E. Teske have speared headed the development of AgDISPpro If there are other authors, they declare that they have no known competing financial interests or personal relationships that could have appeared to influence the work reported in this paper.

Acknowledgements

This work was funded by Bayer, Crop Science Division. We are grateful to Bill Reynolds (LeadingEdge Aerial Technologies) for providing the information required for modeling the PV22X and PV35 UAVs flow fields in CHARM. We would like to thank Dr. Dwayne Moore from Stone Environmental Inc. for reviewing and editing this manuscript.

Appendix A. Supplementary data

Supplementary data to this article can be found online at https://doi.org/10.1016/j.scitotenv.2025.178725.

Data availability

Data will be made available on request.

References

ASABE, 2012.ASAE S327.4 JUL2012 (R2021): terminology and definitions for application of crop or forestry production and protection agents. https://webstore.ansi.org/standards/asabe/asaes327jul2012r2021. Accessed on November 29 2023.

Bilanin, A.J., Teske, M.E., Barry, J.W., Ekblad, R.B., 1989. AGDISP: the aircraft spray dispersion model, code development and experimental validation. Trans. ASAE 32 (1), 327–334. https://doi.org/10.13031/2013.31005.

Bilanin, A.J., Teske, M.E., Hirsh, J.E., 1978. Neutral atmospheric effects on the dissipation of aircraft vortex wakes. AIAA J. 16 (9), 956–961. https://doi.org/10.2514/3.60990.

Bilanin, A.J., Teske, M.E., Williamson, G.G., 1977. Vortex interactions and decay in aircraft wakes. AIAA J. 15 (2), 250–260. https://doi.org/10.2514/3.7318.

Bliss, D.B., Dadone, L., Wachspress, D.A., 1987b. Rotor wake modeling for high speed applications. Proceedings of the 43rd annual forum of the am. Heli. Soc., St. Louis, Missouri. 17-33.

Bliss, D.B., Teske, M.E., Quackenbush, T.R., 1987a. A new methodology for free wake analysis using curved vortex elements. NASA-CR-3958.

Bonds, J., 2022 Jan. A. S., Fritz, B. K., Thistle, H.W. 2022. A field programme for the spray distribution of unmanned aerial spray systems (UASS) and the development of larvicide systems for vector control. Proc. Int. Advances in Pesticide Application. 10, 105–115.

Bonds, J.A.S., Fritz, B.K., Thistle, H.W., Reynolds, B., 2023. Calculation of swath width and swath displacement for uncrewed aerial spray systems. J. ASABE. 66 (3), 523–532. https://doi.org/10.13031/ja.15400.

Cramer, H.E., Bjorklund, J.R., Record, F.A., Dumbauld, R.K., Swanson, R.N., Faulkner, J. E., Tingle, A.G., 1972. Development of dosage models and concepts. In: DTC-TR-72-609-1. Utah, Dugway, US Army Dugway Proving Ground, Dugway.

del Cerro, J., Cruz Ulloa, C., Barrientos, A., de León Rivas, J., 2021. Unmanned aerial vehicles in agriculture: A survey. Agronomy 11 (2), 203. https://doi.org/10.3390/agronomy11020203.

Donaldson, C. duP., Bilanin, A.J., 1975. Vortex wakes of conventional aircraft. AGARDograph No. 204. NATO Advisory Group for Aerospace Research and Development.

Duan, B., Yendol, W.G., Mierzejewski, K., Reardon, R., 1992. Validation of the AGDISP aerial spray deposition prediction model. Pestic. Sci. 36, 19–26. https://doi.org/10.1002/ps.2780360104.

Dubuis, P.H., Droz, M., Melgar, A., Zürcher, U.A., Zarn, J.A., Gindro, K., König, S.L.B., 2023. Environmental, bystander and resident exposure from orchard applications using an agricultural unmanned aerial spraying system. Sci. Total Environ. 10, 163371. https://doi.org/10.1016/j.scitotenv.2023.163371.

Dumbauld, R.K., Borklund, J.R., Saterlie, S. F., 1980. Computer model for predicting aircraft spray dispersion and deposition above and within forest canopies. User Manual for the FSCBG Computer Program, 80–11. USDA Forest Service, Davis, CA.

Felkers E, Kuster C.J., Hamacher G., Anft T., Kohler M., 2024. Pesticide exposure of operators during mixing and loading a drone: towards a stratified exposure assessment. Pest Manag. Sci. doi: https://doi.org/10.1002/ps.8574. (Epub ahead of print).

Fritz, B.K., Martin, D.E., 2020. Measurement and analysis methods for determination of effective swath width from unmanned aerial vehicles. In: Elsik, C.M. (Ed.), Pesticide Formulation and Delivery Systems: 40th Volume, Formulation, Application and Adjuvant Innovation. ASTM International, West Conshohocken, PA, pp. 62–85. https://doi.org/10.1520/STP162720190132.

Glaser, M., Ruppert, F., Becker, M., Stephan, F., Rainer, K., Herbst, A., 2020. Results of the Measurements for Drift in the Application with Unmanned Aerial Vehicles (UAV).

Guebsi, R., Mami, S., Chokmani, K., 2024. Drones in Precision Agriculture: A Comprehensive Review of Applications, Technologies, and Challenges. Drones 8 (11), 30. https://doi.org/10.3390/drones8110686.

Hassler, S.C., Baysal-Gurel, F., 2019. Unmanned aircraft system (UAS) technology and applications in agriculture. Agronomy 9 (10), 618. https://doi.org/10.3390/agronomy9100618.

Herbst, A., Bonds, J., Wang, Z., Zeng, A., He, X., Goff, P., 2020. The influence of unmanned agricultural aircraft system design on spray drift. J. Kult. 72 (1), 1–11. https://doi.org/10.5073/JfK.2020.01.01.

Houbolt, J.C., Steiner, R., Pratt, K.G., 1964. Dynamic Response of Airplanes to Atmospheric Turbulence Including Flight Data on Input and Response. NASA TR R-199: Langley, VA.

International Organization for Standardization (ISO). 2005. Equipment for crop protection — Methods for field measurement of spray drift (ISO Standard No. 22866: 2005).

Kaivosoja, J., 2022. Future possibilities and challenges for UAV-based imaging development in smart farming. In: Lipping, T., Linna, P., Narra, N. (Eds.), New Developments and Environmental Applications of Drones. Springer International Publishing, Cham, pp. 109–119.

Konert, A., Balcerzak, T., 2021. Military autonomous drones (UAVs) from fantasy to reality. Legal and ethical implications. Transp. Res. Procedia 59, 292299. https://doi.org/10.1016/j.trpro.2021.11.121.

Kuster, C. J. , Kohler, M., Hovinga S., Timmermann, C., Hamacher, G., Buerling, K., Chen, L., Hewitt, N.J., Anft, T., 2023. Pesticide exposure of operators from drone application: A field study with comparative analysis to handheld data from exposure models; ACS Agric. Sci. Technol. 2023, 3, 12, 1125–1130. doi:https://doi.org/10.1021/acsagscitech.3c00253.

Langmuir, I., Blodgett, K.B., 1949. A Mathematical Investigation of Water Droplet Trajectories. Report No. RL225,. General Electric Company, Schenectady, NY.

Martin, D.E., Perine, J.W., Grant, S., Abi-Akar, F., Henry, J.L., Latheef, M.A., 2025. Spray deposition and drift as influenced by wind speed and spray nozzles from a remotely piloted aerial application system. Drones 9 (1), 66. https://doi.org/10.3390/drones9010066.

Martin, D.E., Tang, Z., Yang, Y., Latheef, M.A., Fritz, B.K., Kruger, G., Houston, T., 2024. Spray drift characterization of a remotely piloted aerial application system. Appl Engr in Ag 40 (4), 385–399. https://doi.org/10.13031/aea.15605.

Martinez-Guanter, J., Agüera, P., Agüera, J., Pérez-Ruiz, M., 2020. Spray and economics assessment of a UAV-based ultra-low-volume application in olive and citrus orchards. Precis. Agric. 21, 226–243. https://doi.org/10.1007/s11119-019-09665-7.

Miller, P. C. H., Hadfield, D. J., 1989.A Simulation model of the spray drift from hydraulic nozzles. J. Agric. Eng. Res. 42(2), 135–147. doi:https://doi.org/10.1016/0021-8634(89)90046-2.

Nuyttens, D., Baetens, K., De Schampheleire, M., Sonck, B., 2007. Effect of nozzle type, size and pressure on spray droplet characteristics. Biosyst. Eng. 97, 333–345. https://doi.org/10.1016/j.biosystemseng.2007.03.001.

OECD, 2021. Report on the state of the knowledge – literature review on unmanned aerial spray Systems in Agriculture, OECD series on pesticides, no. 105, OECD publishing, Paris.
Quackenbush, T., Bliss, D., 1988. Free wake calculation of rotor flow fields for interactional aerodynamics. Proceedings of the 44th annual forum of the am. Heli. Soc., Washington, D. C. 29-43.
Quackenbush, T.R., Bliss, D.B., 1990. Free wake flow field calculations for rotorcraft interactional dynamics. Vertica 14 (3), 313–327.
Quackenbush, T.R., Bliss, D.B., 1991. Prediction of high-resolution flowfields for rotorcraft aeroacoustics. AIAA J. 29 (11), 1778–1786. https://doi.org/10.2514/3.10804.
Quackenbush, T.R., Bliss, D.B., Wachspress, D.A., 1989. New free-wake analysis of rotorcraft hover performance using influence coefficients. J. Aircr. 26 (12), 1090–1097.
Quackenbush, T.R., Boschitsch, A.H., Wachspress, D.A., 1996. Fast Analysis Methods for Surface-Bounded Flows with Applications to Rotor Wake Modeling, Proceedings of the 52nd Annual Forum of the am. Heli. Soc, Washington, D. C, pp. 1514–1531.
Quackenbush, T.R., Lam, C.-M.G., Bliss, D.B., 1994. Vortex methods for the computational analysis of rotor/body interaction. J. Am. Helic. Soc. 39 (4), 14–23. https://doi.org/10.4050/JAHS.39.14.
Quackenbush, T.R., Wachspress, D.A., Boschitsch, A.H., 1995. Rotor aerodynamic loads computation using a constant vorticity contour free wake model. J. Aircr. 32 (5), 911–920. https://doi.org/10.2514/3.46818.
Quackenbush, T.R., Wachspress, D.A., Boschitsch, A.H., Curbishley, T.B., 1999. A Comprehensive Hierarchical Aeromechanics Rotorcraft Model (CHARM) for General Rotor/Surface Interaction. Continuum Dynamics, Inc. Report No. 99–03.
Quackenbush, T.R., Whitehouse, G.R., Silbaugh, B.S., Danilov, P.V., 2017. Analysis of download and rotor/airframe interactions in hover. Proceedings of the 73rd annual forum of the am. Heli. Soc., Fort Worth. https://doi.org/10.4050/F-0073-2017-12019. TX. 1-15.
R Core Team, 2022. R: A Language and Environment for Statistical Computing. R Foundation for Statistical Computing, Vienna, Austria. https://www.R-project.org/.
Radoglou-Grammatikis, P., Sarigiannidis, P., Lagkas, T., Moscholios, I., 2020. A compilation of UAV applications for precision agriculture. Comput. Netw. 172, 107148. https://doi.org/10.1016/j.comnet.2020.107148.
Reed, W.H., 1953. An analytical study of the effect of airplane wake on the lateral dispersion of aerial spray. In: NACA 3032. VA, Langley.
Rice, A., Hewitt, A., Reynolds, B., Brayden, B., Mitchell, R., Hanzas, J., Toth, B., Arpino, M., 2022. Comparison of drift deposition from a UAS application using tracer dye with multiple downwind sampling methodologies. ACS Fall 2022 Conference, Chicago, IL.
Rule, J.A., Bliss, D.B., 1995. Prediction of turbulent trailing vortex structure for rotorcraft blade vortex interaction. In: Proceedings of the 51st Annual Forum of the am. Fort Worth, TX, Heli. Soc.
Rule, J.A., Bliss, D.B., 1998. Prediction of viscous trailing vortex structure from basic loading parameters. AIAA J. 36 (2), 208–218. https://doi.org/10.2514/2.7503.
Sahni, R.K., Kumar, S.P., Thorat, D., Rajwade, Y., Jyoti, B., Ranjan, J., Anand, R., 2024. Drone spraying system for efficient agrochemical application. In Chouhan, S.S, Sing, P. (Eds), Precision Agriculture. Applications of Computer Vision and Drone Technology in Agriculture 4.0. Springer. doi:https://doi.org/10.1007/978-981-99-8684-2.
Sharkey, N., 2011. The automation and proliferation of military drones and the protection of civilians. Law Innov. Technol. 3, 229–240. https://doi.org/10.5235/175799611798204914.
Technologies, Leading Edge Aerial, 2023. PrecisionVision 35X. https://leaaerialtech.com/precisionvision-35x.
Teske, M.E., Bilanin, A.J., Barry, J.W., 1993a. Decay of aircraft vortices near the ground. AIAA J. 31 (8), 1531–1533. https://doi.org/10.2514/3.49087.
Teske, M.E., Bowers, J.F., Rafferty, J.E., Barry, J.W., 1993b. FSCBG: an aerial spray dispersion model for predicting the fate of released material behind aircraft. Environ. Toxicol. Chem. 12 (3), 453–464. https://doi.org/10.1002/etc.5620120307.
Teske, M.E., Thistle, H.W., 2003. Release height and far-field limits of Lagrangian aerial spray models. Trans. ASAE 46 (4), 977–983. https://doi.org/10.13031/2013.13953.
Teske, M.E., Thistle, H.W., Fritz, B., 2019. Modeling aerially applied sprays: an update to AGDISP model development. Trans. ASABE 62 (2), 343–354. https://doi.org/10.13031/trans.13129.
Teske, M.E., Thistle, H.W., Ice, G.G., 2003. Technical advances in modeling aerially applied sprays. Trans. ASAE 46 (4), 985–996. https://doi.org/10.13031/2013.13955.
Teske, M.E., Thistle, H.W., Londergan, R.J., 2011a. Modification of droplet evaporation in the simulation of fine droplet motion using AGDISP. Trans. ASABE 54 (2), 417–421. https://doi.org/10.13031/2013.36444.
Teske, M.E., Thistle, H.W., Riley, C.M., Hewitt, A.J., 2018a. Laboratory measurements of evaporation rate of droplets at low relative wind speed. Trans. ASABE 61 (3), 919–923. https://doi.org/10.13031/trans.12743.
Teske, M.E., Thistle, H.W., Schou, W.C., Miller, P.C.H., Strager, J.M., Richardson, B., Butler Ellis, M.C., Barry, J.W., Twardus, D.B., Thompson, D.G., 2011b. A review of computer models for pesticide deposition prediction. Trans. ASABE 54 (3), 789–802. https://doi.org/10.13031/2013.37094.
Teske, M.E., Wachspress, D.A., Thistle, H.W., 2018b. Prediction of aerial spray release from UAVs. Trans. ASABE 61 (3), 909–918. https://doi.org/10.13031/trans.12701.
Teske, M.E., Whitehouse, G.R., 2022. Predicting the aerial application of dispersant onto an oil spill. ASME Open J. Engr. 011052-1. https://doi.org/10.1115/1.4055984.
Teske, M.E., Whitehouse, G.R., 2024. Modeling aerially applied sprays: additional AGDISPpro model comparisons. J. ASABE 67 (6), 1509–1519. https://doi.org/10.13031/ja.15907.
Teske, M.E., Whitehouse, G.R., Curbishley, T.B., 2022. Development and validation of a sprayer-based software system for drift reduction and dispersion prediction. Appl. Engr. Ag. 38 (2), 435–444. https://doi.org/10.13031/aea.15009.
Thistle, H.W., Teske, M.E., Richardson, B., Strand, T.M., 2020. Technical note: model physics and collection efficiency in estimates of pesticide spray drift model performance. Trans. ASABE 63 (6), 1939–1945. https://doi.org/10.13031/trans.14024.
Turner, D.B., 1994. Workbook of Atmospheric Dispersion Estimates: An Introduction to Dispersion Modeling. Lewis Publishers, Boca Raton, FL.
Wachspress, D.A., Quackenbush, T.R., 2001. BVI noise predictions using a comprehensive rotorcraft analysis. In: Proceedings of the 57th Annual Forum of the am. Washington, D.C, Heli. Soc.
Wachspress, D.A., Quackenbush, T.R., 2006. Impact of rotor design on coaxial rotor performance, wake geometry and noise. In: Proceedings of the 62nd Annual Forum of the am. Phoenix, AZ, Heli. Soc., 23 pages.
Wachspress, D.A., Quackenbush, T.R., Boschitsch, A.H., 2003a. First principles free vortex wake analysis for helicopters and tiltrotors. Proceedings of the 59th Annual Forum of the American Helicopter Society. 59 (2), 1763–1786.
Wachspress, D.A., Quackenbush, T.R., Boschitsch, A.H., 2003b. Rotorcraft interactional aerodynamics with fast panel/fast vortex methods. J. Am. Helic. Soc. 48 (4), 223–235. https://doi.org/10.4050/JAHS.48.223.
Wachspress, D.A., Quackenbush, T.R., Boschitsch, A.H., A.H., 2003c. Rotorcraft interactional aerodynamics with fast vortex/fast panel methods. J. Am. Heli. Soc. 48 (4), 223–235. https://doi.org/10.4050/JAHS.48.223.
Wachspress, D.A., Whitehouse, G.R., Keller, J.D., Yu, K., 2009. A high fidelity brownout model for flight simulations and trainers. In: Proceedings of the 65th Annual Forum of the am. Grapevine, TX, Heli. Soc., 24 pages.
Wang, C., Herbst, A., Zeng, A., Wongsuk, S., Qiao, B., Qi, P., Bonds, J., Overbeck, V., Yang, Y., Gao, W., He, X., 2021. Assessment of spray deposition, drift and mass balance from unmanned aerial vehicle sprayer using an artificial vineyard. Sci. Total Environ. 777, 146181. https://doi.org/10.1016/j.scitotenv.2021.146181.
Wang, C.L., Zeng, A.J., He, X.K., Song, J.L., Herbst, A., Gao, W., 2020a. Spray drift characteristics test of unmanned aerial vehicle spray unit under wind tunnel conditions. Int J Agric & Biol Eng 13, 13–21. https://doi.org/10.25165/j.ijabe.20201303.5716.
Wang, G., Han,Y., Li, X., Andaloro, J., Chen, P., Hoffmann, W.C., Han, X., Chen, S., Lan, Y., 2020b. Field evaluation of spray drift and environmental impact using an agricultural unmanned aerial vehicle (UAV) sprayer. Sci. Total Environ., 737. 139793. doi:https://doi.org/10.1016/j.scitotenv.2020.139793.
Weicai, Q., Panya, C., 2023. Analysis of the research progress on the deposition and drift of spray droplets by plant protection UAVs. Sci. Rep. 13, 14935. https://doi.org/10.1038/s41598-023-40556-0.
Whitehouse, G.R., Boschitsch, A.H., Quackenbush, T.R., Wachspress, D.A., Brown, R.E., 2007. Novel eulerian vorticity transport wake module for rotorcraft flow analysis. In: Proceedings of the 63rd Annual Forum of the am. Virginia Beach, VA, Heli. Soc., 16 pages.
Whitehouse, G.R., Wachspress, D.A., Quackenbush, T.R., 2018. Predicting the influence of blade shape on hover performance with comprehensive analyses. J. Aircr. 55 (1), 111–121. https://doi.org/10.2514/1.C034073.
Willmott, C.J., 1981. On the validation of models. Phys. Geogr. 2, 184–194.
Wongsuk, S., Zhu, Z., Zheng, A., Qi, P., Li, Y., Huang, Z., Han, H., Wang, C., He, X., 2024. Assessing the potential spray drift of a six-rotor unmanned aerial vehicle sprayer using a test bench and airborne drift collectors under low wind velocities: impact of atomization characteristics and application parameters. Pest Manag. Sci. 80 (12), 6053–6067. https://doi.org/10.1002/ps.8334 (Epub 2024 Jul 19).
Yan, X., Zhou, Y., Liu, X., Yang, D., Yuan, H., 2021. Minimizing occupational exposure to pesticide and increasing control efficacy of pests by unmanned aerial vehicle application on cowpea. Appl. Sci. 11 (20), 9579. https://doi.org/10.3390/app11209579.
Yang, F., Xue, X., Cai, C., Sun, Z., Zhou, Q., 2018. Numerical simulation and analysis on spray drift movement of multirotor plant protection unmanned aerial vehicle. Energies 11 (9), 2399. https://doi.org/10.3390/en11092399.
Zhang, R., Hewitt, A.J., Chen, L., Li, L., Tang, Q., 2023. Challenges and opportunities of unmanned aerial vehicles as a new tool for crop pest control. Pest Manag. Sci. 79 (11). https://doi.org/10.1002/ps.7683. Pages4123-4131.
Zhou, W., 2013. Application and popularization of agricultural unmanned plant protection helicopter. Agric. Eng. 3 (S1), 56–58.